

# *decryst*: an efficient software suite for structure determination from powder diffraction

Yu Liu <caspervector@gmail.com>

National Laboratory for Superconductivity, Institute of Physics, Chinese Academy of Sciences, Beijing 100190, People's Republic of China; University of Chinese Academy of Sciences, Beijing 100149, People's Republic of China

## Synopsis

Keywords: incremental computation; parallel and distributed computing; powder diffraction; structure determination; computer program.

*decryst* is an open source software suite for structure determination from powder diffraction using the direct space method, which can apply anti-bump constraints automatically in global optimisation using the efficient algorithm by Liu (2017). *decryst* can offer high performance due to the application of incremental computation, and is designed with parallel and distributed computing in mind.

## Abstract

Presented here is *decryst*, a software suite for structure determination from powder diffraction, which uses the direct space method, and is able to apply anti-bump constraints automatically and efficiently during the procedure of global optimisation using the crystallographic collision detection algorithm by Liu (2017). *decryst* employs incremental computation in its global optimisation cycles, which results in dramatic performance enhancement; it is also designed with parallel and distributed computing in mind, allowing for even better performance by simultaneous use of multiple processors. *decryst* is free and open source software, and can be obtained at <https://gitlab.com/CasperVector/decryst/>; it strives to be simple yet flexible, in the hope that the underlying techniques could be adopted in more crystallographic applications.

## 1 Introduction

In structure determination from powder diffraction (SDPD) (David, Shankland, McCusker & Baerlocher 2002), the reciprocal space methods, *eg.* direct methods (not to be confused with the direct space method), Patterson synthesis and charge flipping (Baerlocher, McCusker & Palatinus 2006), work by extracting the amplitudes of structure factors for individual reflections and then phasing the reflections; they usually require high resolution diffraction data, which can be difficult or impossible to obtain under certain circumstances. In contrast, the direct space method (Černý & Favre-Nicolin 2007) works by using global optimisation algorithms to find a coordinate combination for independent atoms in the unit cell that minimises an objective function, with the most important part of the function being the divergence between the originally observed diffraction pattern and the pattern computed from the coordinates, usually measured by the Bragg  $R$  factor; it is better at processing low resolution data and solving molecular crystals.

However, as noted by Liu (2017), even for structures as simple as  $\text{PbSO}_4$ , there can exist several obviously unreasonable crystallographic models with  $R$  factors comparable to (or even smaller than) that of the correct model, and most of them have some bumping atom pairs. In the direct space method, it is desirable to automatically eliminate these unreasonable models during the procedure of global optimisation, which requires real-time crystallographic collision detection. Liu (2017) presented a generic algorithm for this, and proposed an evaluation function for atom bumping; based on this research, we developed *decryst*, a SDPD software suite, which is the subject of this article.

Inspired by the *make* utility (Feldman 1979), which identifies the pieces of a project that have changed, and then executes commands to rebuild these pieces (Figure 1), we applied incremental computation in *decryst*, resulting in a dramatic speedup of the global optimisation procedure. But the speedup from incremental computation is still limited when there are too many independent coordinates to be determined, because the size of the search space grows exponentially with regard to the degree of freedom (DOF). Since computers with multiple processors are the norm today, we designed *decryst* with parallel and distributed computing in mind, to further enhance its performance by employing multiple processors simultaneously.

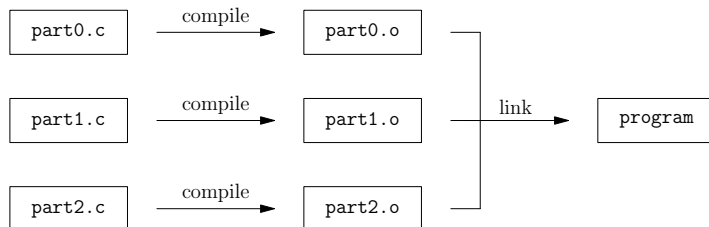


Figure 1: How *make* builds an example program: after `program` is built, to rebuild it when `part0.c` somehow changes, *make* would only recompile `part0.c` and then relink all `.o` files

## 2 Underlying techniques in *decryst*

### 2.1 *decryst*: an overview

*decryst* is a software suite that attempts to determine the structure of crystals from their indexed powder diffraction data using the typical direct space method summarised by Černý & Favre-Nicolin (2007). It also employs the equivalent position combination (EPC) method (Deng & Dong 2009), so that it can transform the original  $3n$ -dimensional global optimisation problem into multiple smaller and mutually independent optimisation problems: *eg.* for  $\text{PbSO}_4$  ( $Pnma$ ,  $Z = 4$ ), *decryst* transforms the 72-dimensional optimisation problem into 35 small optimisation problems, each corresponding to a single EPC with the DOF ranging from 6 to 12.

Given this background, it is expected that *decryst* would be functionally similar to *EPCryst* (Deng & Dong 2011); however, *decryst* differs from *EPCryst*, most importantly in that it can automatically apply anti-bump constraints using the efficient crystallographic collision detection algorithm by Liu (2017). Additionally, the computational performance of *decryst* is greatly improved over *EPCryst* through, to our knowledge, the first generic application of incremental computation in the global optimisation procedure (*cf.* Subsection 2.2). Moreover, *decryst* is designed with parallel and distributed computing in mind, allowing for further enhancement of the performance (*cf.* Subsection 2.4).

We would like to note that, even without employing incremental computation or parallelism, *decryst* is already vastly faster than *EPCryst*: *eg.* on our computer, global optimisation for the correct EPC of  $\text{PbSO}_4$  requires several seconds with *decryst*, and more than 1000 seconds with *EPCryst*. This is achieved through (1) frugal implementation of algorithms, (2) application of cache-friendly algorithms and data structures (Bryant & O’Hallaron 2011), (3) use of an effective adaptive simulated annealing

schedule (Lam & Delosme 1988), and (4) fast computation of structure factors using the formulae (where  $\vec{q}$  is the scattering vector):

$$F(\vec{q}) = \sum_i f_i(\vec{q})(e^{2\pi i \vec{q} \cdot \vec{x}_i} + e^{2\pi i \vec{q} \cdot (-\vec{x}_i)}) = 2 \sum_i f_i(\vec{q}) \cos(2\pi \vec{q} \cdot \vec{x}_i)$$

(for centrosymmetric cells, where  $i$  is the index of a centrosymmetric atom pair), and

$$F(\vec{q}) = \sum_{ij} f_i(\vec{q}) e^{2\pi i \vec{q} \cdot (\vec{x}_i + \vec{r}_j)} = \sum_i f_i(\vec{q}) e^{2\pi i \vec{q} \cdot \vec{x}_i} \sum_j e^{2\pi i \vec{q} \cdot \vec{r}_j}$$

(for centred cells, where  $\vec{r}_j$  is the coordinates of an origin).

## 2.2 Incremental computation of the objective function

*decryst* uses a linear combination of the Bragg factor

$$R = \sum_{hkl} |I_{\text{obs},hkl} - I_{\text{calc},hkl}| / \sum_{hkl} I_{\text{obs},hkl}$$

and an evaluation function  $B$  for atom bumping as the objective function

$$E = \mu B + (1 - \mu) R / 2,$$

where  $\mu \in [0, 1]$  is the combination factor (Liu 2017). So obviously, in order to speed up the global optimisation procedure, we need to speed up the computation of  $R$  and  $B$ ; and since  $R$  most importantly depends on structure factors, to speed up the computation of  $R$ , we need to speed up the computation of structure factors.

Often, the difference between crystallographic models in two adjacent global optimisation cycles is simply the displacement of one independent atom, so the structure factors in the two cycles are, by additivity of the Fourier transform, subject to the relation

$$F'(\vec{q}) - F(\vec{q}) = \sum_j f_j(\vec{q})(e^{2\pi i \vec{q} \cdot \vec{x}'_j} - e^{2\pi i \vec{q} \cdot \vec{x}_j}),$$

where  $j$  is the index of a moved atom. Using this relation, we are able to incrementally compute structure factors using previously computed structure factors: we only need to recompute the  $\exp(2\pi i \vec{q} \cdot \vec{x}_j)$  term for the moved atoms instead of for all atoms in the unit cell; therefore if there are  $m$  independent atoms in the unit cell, and the atoms are moved in turn between the optimisation cycles, recomputation for all atoms would be distributed into  $m$  cycles (instead of only one cycle), resulting in  $m$  times performance in computation of the structure factor compared with the naïve approach.

Similarly, for atom bumping evaluation functions based on a two-body potential

$$C = \sum_{\{k_0, k_1\}} c(k_0, k_1),$$

where  $c$  is a given two-body function and  $k$  is the index of an atom in the unit cell, it is trivial that  $c(k_0, k_1)$  is only changed for pairs  $\{k_0, k_1\}$  involving a moved atom, so  $C$  can also be computed incrementally: we only need to recheck the collision between these pairs. Remembering that by exploiting the equivalent position symmetry (Liu 2017), we only need to check pairs involving atoms in the asymmetric unit, so the total number of re-tests is  $(n - 1) + (m - 1)(n' - 1)$  (where  $n$ ,  $m$  and  $n'$  are the total number of atoms in the unit cell, the total number of atoms in the asymmetric unit and the number of equivalent atoms of the moved atom, respectively), which would be approximately  $O(n)$  for the average case. Therefore, by employing incremental computation, we no longer need a dedicated broad phase, like sweep and prune, in order to avoid  $O(n^2)$  time complexity in collision

detection, since using the equivalent position symmetry is already sufficient. The evaluation function  $B$  in *decryst* is based on a two-body potential, so this technique is applicable.

We would like to note that when the number of optimisation cycles is large, the accumulation of summation errors from floating point arithmetic can become a serious problem. Incremental floating point summation algorithms like the one by Kahan (1965) are inapplicable, since the mean value of the numbers being summed is asymptotically zero (Higham 1993). For now, *decryst* works around this by internally using fixed point arithmetic, which is free from summation errors, for incremental summations.

### 2.3 Performance evaluation of incremental computation in *decryst*

Apart from those data available at the project homepage <https://gitlab.com/CasperVector/decryst/>, additional test data for this article can be obtained from the supplementary materials. All time consumptions reported in this subsection were measured on an Intel i7-3720QM CPU.

We obtained several crystal structures of varying complexities from the American Mineralogist Crystal Structure Database (Downs & Hall-Wallace 2003). For each structure, we computed the objective function  $E$ , either with or without using incremental computation (corresponding to  $t_{\dots, \text{incr}}$  and  $t_{\dots, \text{orig}}$  in the table, respectively), for 100 groups of crystallographic models, each group consisting of 100 models with random coordinates of the independent atoms. We collected the averages and standard deviations of time consumed in computation of either the entire objective function ( $t_{E, \dots}$ ) or only the Bragg  $R$  factor ( $t_{R, \dots}$ ) for each group divided by the number of models in each group, as shown in Table 1.

Table 1: Results for performance evaluation of incremental computation in *decryst* (all time consumptions are in  $\mu\text{s}$ ): “ID” is the AMCSD database code for the test structure,  $n$  is the total number of atoms in the unit cell,  $m$  is the number of independent atoms,  $N_{\text{refl}}$  is the number of recorded reflections;  $t_{E, \dots}$  and  $t_{R, \dots}$  are time consumed in computation of  $E$  and  $R$  for each model, respectively;  $t_{\dots, \text{incr}}$  and  $t_{\dots, \text{orig}}$  are obtained with and without using incremental computation, respectively

ID	$n$	$m$	$N_{\text{refl}}$	$t_{R, \text{incr}}$	$t_{R, \text{orig}}$	$t_{E, \text{incr}}$	$t_{E, \text{orig}}$
0005558	24	5	94	8.9(3)	43.9(5)	12.5(7)	44.5(7)
0009272	64	8	80	39.7(9)	241(3)	50.6(6)	242(3)
0009563	90	10	76	15.0(2)	168(3)	30.0(7)	174(2)
0002630	126	14	73	11.3(3)	244(3)	30.7(3)	252(2)
0000427	152	20	374	27.4(5)	639(7)	53.6(7)	663(8)
0000447	160	4	32	27.0(9)	87(2)	59(1)	102(2)

From the table we conclude that for many crystal structures, computation of the objective function, including both the Bragg  $R$  factor and the atom bumping evaluation function, can be dramatically (sometimes by an order of magnitude or more) sped up by incremental computation. We note that the time consumptions for “0009272” and  $t_{\dots, \text{orig}}$  for “0000447” might appear anomalous, but actually the former can be explained by the fact that the structure does not have a centred cell and that none of the used Wyckoff positions are centrosymmetric (*cf.* Subsection 2.1), while the latter can be explained by the small  $m$  in comparison with  $n$  (Liu 2017) and the much smaller  $N_{\text{refl}}$  in comparison with those of all other test structures.

### 2.4 Parallelism with *decryst*

Just like *EPCryst*, *decryst* filters out obviously unreasonable EPCs using statistical analyses, and then performs global optimisation on the remaining ones; and since tasks on different EPCs are mutually independent, *decryst* performs them in parallel (Figure 2(a)). As a result from parallel processing of

tasks on different EPCs, *decryst*'s ability for structure determination is greatly improved over *EPCryst*. As Deng & Dong (2011) noted, “*EPCryst* works particularly well when the number of generated TSMs is small (say less than 100) and the number of parameters is not greater than ten” (a “TSM” is a trial structure model corresponding to a single EPC); in contrast, by distributing the tasks among multiple processors, and applying previously discussed performance optimisation techniques, *decryst* can handle thousands of EPCs, each with a DOF more than 20. Noticing the large number of possible EPCs and the dramatic reduction in the DOF resulted from the EPC method in most useful cases, we expect the parallelisation of EPC tasks to offer huge opportunities.

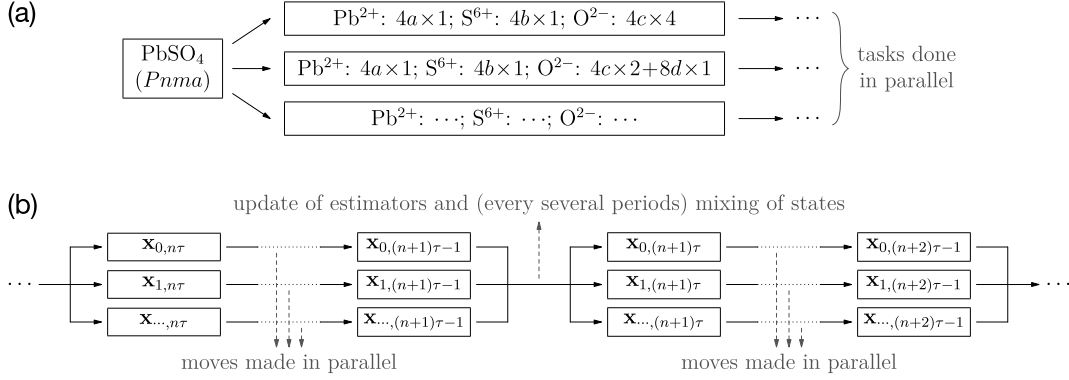


Figure 2: Two types of parallelism in *decryst*: (a) parallel processing of tasks on different EPCs; (b) parallelisation of the simulated annealing algorithm

For EPCs with large DOFs, *decryst* can also perform parallel global optimisation: it uses the parallel simulated annealing algorithm by Chu, Deng & Reinitz (1999), which is based on the adaptive annealing schedule by Lam & Delosme (1988). The Lam schedule uses continuous cooling, with the cooling rate dynamically computed from several statistical estimators gathered periodically (every  $\tau$  cycles); for best performance, the average move size is also dynamically controlled, to keep the acceptance ratio of the moves around 0.44. Chu et al. (1999) noted that the underlying physical metaphor of simulated annealing is the sampling of Boltzmann distributions, and that multiple sampling processes can be correlated by periodic mixing of the latest states from all processes (Figure 2(b)), with the probability for choosing a state under temperature  $T$  being

$$p_j = \exp(-E_j/T) / \sum_j \exp(-E_j/T),$$

where  $E_j$  is the value of the objective function on process  $j$ . Using this technique, the sampling procedure can be distributed among multiple processes, hence enabling parallelism in simulated annealing.

For our application, we made some minor adjustments to the original algorithms:

- Due to the periodic boundary of the unit cell, we model the search domain of the coordinate combination as a hyperrectangle with a periodic boundary instead of an infinite search domain as in the original algorithms. Accordingly, the move size is generated from a random-signed wrapped exponential distribution instead of a random-signed exponential distribution.
- Since the coordinate combination is randomly initialised, initial cycles at infinite temperature used to erase the initial state are no longer needed. Similarly, because we have a dedicated statistical analysis stage for EPCs, initial cycles used to gather statistics for initialisation of the statistical estimators are no longer necessary.

## 3 Applications of *decryst*

### 3.1 *decryst*: the programs

*decryst* is free and open source software that runs on Unix-like operating systems, and can be obtained at <https://gitlab.com/CasperVector/decryst/>. Realising that we cannot afford to “reinvent the wheel” with our limited resource, we implemented *decryst* in a simple yet flexible way. We explicitly wish the techniques in *decryst* to be examined by fellow crystallographers, and eventually be adopted in more applications; we believe this will hopefully result in significantly better performance of crystallographic software in general.

*decryst* is composed of multiple parts (Figure 3(a); details on invocation of individual programs and their input formats have been provided at the project homepage, and can be freely accessed):

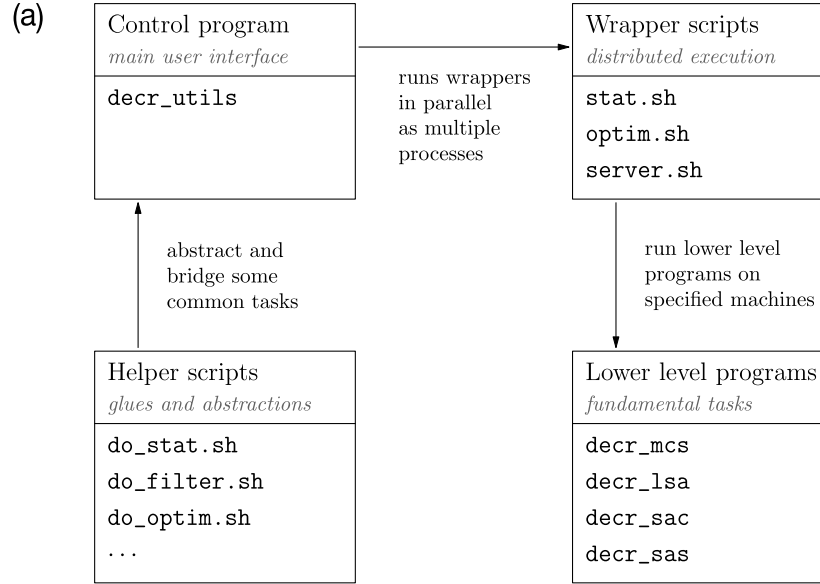
- Several single-purpose lower level programs, each of which implements one basic functionality (statistical analyses, global optimisation); they are written in C to achieve high performance. These programs and the control program introduced below comprise the core of *decryst*.
- One higher level multi-purpose program that controls the lower level programs; this program is written in Python for maximal flexibility. Some functionalities (and in particular, enumeration of EPCs), which are fairly complex but not performance-critical, are also implemented in this program.
- Wrapper scripts that invoke a lower level program on a specified machine according to some control parameters. When the control program performs a task, it actually runs wrapper scripts in parallel, resulting in specified lower level programs to be executed on specified machines in parallel, hence enabling parallel and distributed computing.
- Helper scripts that bridge different tasks and provide higher abstractions, *eg.* one that filters the list of EPCs for use in global optimisation according to the results of statistical analyses using a figure of merit like the one by Deng & Dong (2011). Helpers and wrappers are written as Unix shell scripts.

*decryst* uses textual interfaces (*eg.* the input format for the control program as shown in Figure 3(b)) that are friendly to standard Unix text processing utilities. This design allows *decryst* to perform highly automated tasks exactly at the will of the user; as an example for this, we solved the “0009563” structure in Table 1. All time consumptions reported in this section were measured on an Intel i7-3720QM CPU; the procedure has been provided at the project homepage, and detailed results can be obtained from the supplementary materials.

### 3.2 “0009563”: solving the heavy atoms

From the indexed XRD data (*decryst* merges the intensities for reflections that overlap in  $2\theta$ , so the data were treated as regular powder diffraction data) for “0009563” obtained from AMCSD, we are able to tell that the formula for its  $P\bar{3}c1$  unit cell is  $\text{Rb}_{12}\text{Ti}_6\text{Ge}_{18}\text{O}_{54}$ . Since all metal atoms in this structure are much heavier than  $\text{O}^{2-}$ , it is suitable to solve the structure using the heavy atom method. After commenting out lines in the input file involving the  $\text{O}^{2-}$  atoms (*cf.* Figure 3(b)), we instructed *decryst* to enumerate all possible EPCs for the heavy atoms according to the input file, resulting in 1451 EPCs in total.

Before attempting to actually solve the heavy atoms, it is very useful to filter out the unreasonable EPCs using certain criteria. In early works, *eg.* those by Lu & Liang (1965) and Reddy, Storm & Knox (1965), for simple crystals, crystallographers were able to identify EPCs that are bound to produce crystallographic models with atom bumping regardless of the independent atoms’ coordinates by skillful analyses of the geometric properties of the EPCs. Using the atom bumping evaluation function  $B$  (*cf.* Subsection 2.2), we can perform the same task programmatically in *decryst*: by setting



(b)

```

# (Lines beginning with '#' are comments and are ignored.)
# ID of space group, (a, b, c), (alpha, beta, gamma).
167a    4.7602 4.7602 12.9933   90 90 120
# Combination factor 'mu', and some other control parameters.
0.25 0.75 0.875 0.5 1.0
# Global EPC constraints ('--' for the defaults).
--

# Atom species, number of atoms, EPC constraints, already
# guessed EPCs with unknown coordinates ('--' for none).
Al3+    12    --    --
O2-     18    --    --
# Pairwise zoom factors (here says "1.6 for Al3+/Al3+ pairs").
1.6:0-0
# Wyckoff positions and coordinates for already solved atoms
# (here says "one Al3+ at one 12c site: (0, 0, 0.14784)").
O@c1    0      0      0.14784

# Data for individual reflections:
# 2-theta, FWHM, hkl, multiplicity, intensity.
25.59   0.2    0 1 2   6      61.91
35.17   0.2    1 0 4   6      96.62
# (... further data lines left out for brevity ...)
  
```

Figure 3: (a) Organisation of individual programs in *decryst*; (b) an example input file for *decryst*'s control program (for  $\text{Al}_2\text{O}_3$ , with AMCSD database code "0009325")

the combination factor  $\mu$  to 0.99 (we deliberately avoided using 1 exactly, so that the optimisation algorithm would not terminate too early with EPCs that produced models with  $B = 1$  with a big probability) before running global optimisation on the EPCs, we were able to find those EPCs that were incapable of producing models free from bumping at all.

After examining the results from the previous global optimisation step, we dropped all EPCs with final  $E > 0.12$ , leaving 183 (13%) EPCs as candidates for the next step. We then restored the original  $\mu$  for these EPCs, and again performed global optimisation on them; since these EPCs had DOFs ranging from 5 to 8, and only involved heavy atoms, the results were quite reproducible, so we only ran global optimisation once for each EPC. After examining the results, we discarded the EPCs with final  $E > 0.2$ , leaving 26 EPCs for the heavy atoms; noticing that the  $B$  values for these EPCs clearly fell into two different groups, one with the greatest  $B = 0.0027$  and the other with  $B$  ranging from 0.056 to 0.112, we dropped all EPCs with  $B > 0.02$ , leaving 20 (11%) of them.

By enabling parallelism in *decryst* (achieved by specifying appropriate control parameters in a “hosts” file), we were able to make full use of all 8 available CPU threads. With parallelism enabled, the procedures (excluding human intervention) in this subsection took about 2.5 minutes to complete. As a matter of fact, the heavy atoms were solved correctly in this step: the correct EPC ( $\text{Rb}^+$ :  $12g \times 1$ ;  $\text{Ti}^{4+}$ :  $2b \times 1 + 4d \times 1$ ;  $\text{Ge}^{4+}$ :  $6f \times 1 + 12g \times 1$ ) had the smallest  $E = 0.058$ , and was solved correctly; visual inspection of solutions for the 6 EPCs rejected due to large  $B$  values confirmed that they all had obviously bumping atom pairs.

### 3.3 “0009563”: solving the $\text{O}^{2-}$ atoms

*decryst* can automatically merge solutions with the input file to produce new input files for solved EPCs with all comments preserved, as well as CIF files for the (partially) solved structures. After merging the solutions for the candidate EPCs from the previous step, we uncommented the  $\text{O}^{2-}$  lines in all these input files, and enumerated full EPCs based on the previously chosen EPCs for the heavy atoms, resulting in 4455 EPCs in total. Then again we attempted to identify the unreasonable ones among these EPCs using the function  $B$  by temporarily setting  $\mu = 0.99$ : in order to save time, we filtered out all EPCs with smallest  $E > 0.99$  after the statistical analyses step, resulting in only 2186 (49%) EPCs remaining; after the global optimisation step, we dropped the EPCs with final  $E > 0.05$ , leaving 110 (5%) candidates for the next step.

Considering that the DOFs for these EPCs were mainly 10 to 13, and that  $\text{O}^{2-}$  has very limited contribution to the diffraction pattern of “0009563”, the results from global optimisation on these EPCs were expected to vary from run to run, so we needed to perform global optimisation several times on the EPCs and pick the plausible solutions. In order to reduce the number of candidates for visual inspection, we gradually reduced the number of results after the runs: after the first run, we dropped all EPCs with final  $B > 0.02$ , leaving 50 EPCs; after the second run, we chose the 20 EPCs with smallest  $E$  values; after the third run, we chose the top 10 EPCs. It was retroactively confirmed that the final candidates usually had the smallest  $E$  values in these runs.

For each of the 10 remaining EPCs, we performed global optimisation 10 times; among the 100 solutions, we discarded those with  $B > 0.02$ , leaving 90 of them, and then visually inspected the remaining solutions. Crude inspection showed that the correct EPC (with  $\text{O}^{2-}$  at  $6f \times 1 + 12g \times 4$ ) was a clear winner, since all solutions from other EPCs had ill-defined bonding relations: patently uneven coordination numbers for the same kind of atoms (Figure 4(c)), metal atoms occupying sites with too many metallic neighbours in the presence of lone  $\text{O}^{2-}$  atoms in the unit cell (Figure 4(d)), *etc.* Noticing that this EPC also produced the 10 solutions with smallest  $E$  values among all 100 solutions, it was without doubt the only plausible EPC for “0009563”.

Among the 10 solutions from this EPC, we found two distinct plausible ones: one of them (Figure 4(a)) was very close to the originally reported structure, and only needed some refinement; the other (Figure 4(b)) did not appear immediately incorrect, but  $\text{Ge}^{4+}$  atoms in the structure had quite painful coordination polyhedra. With parallelism enabled, the procedures (excluding human intervention) in this subsection took 25 minutes in total.



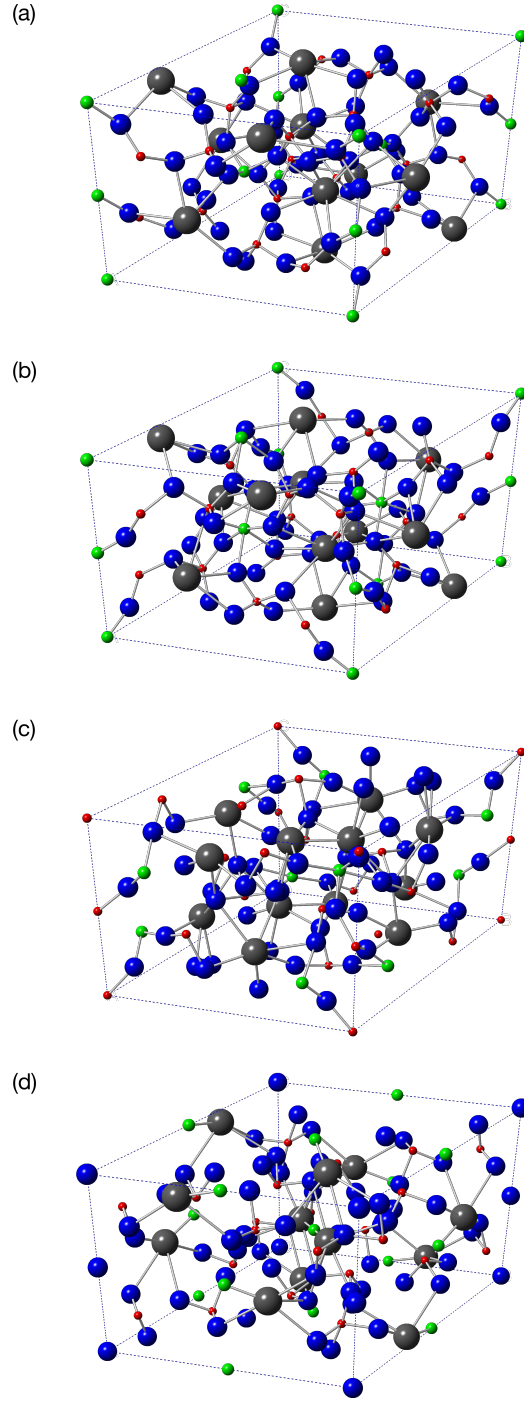


Figure 4: Some solutions for “0009563”: (a) the one closest to the correct solution, from EPC [ $\text{Rb}^{+}$ :  $12g \times 1$ ;  $\text{Ti}^{4+}$ :  $2b \times 1 + 4d \times 1$ ;  $\text{Ge}^{4+}$ :  $6f \times 1 + 12g \times 1$ ;  $\text{O}^{2-}$ :  $6f \times 1 + 12g \times 4$ ]; (b) the other plausible one, from the same EPC as (a), but with painful coordination polyhedra for the  $\text{Ge}^{4+}$  atoms; (c) one with each  $\text{Ge}^{4+}$  atom on a cell edge coordinated by 6  $\text{O}^{2-}$  atoms and each of the rest coordinated by 3  $\text{O}^{2-}$  atoms, from EPC [ $\text{Rb}^{+}$ :  $12g \times 1$ ;  $\text{Ti}^{4+}$ :  $6f \times 1$ ;  $\text{Ge}^{4+}$ :  $2b \times 1 + 4d \times 1 + 12g \times 1$ ;  $\text{O}^{2-}$ :  $6f \times 1 + 12g \times 4$ ]; (d) one with each  $\text{Ti}^{4+}$  atom coordinated by 2  $\text{Rb}^{+}$  atoms in the presence of lone  $\text{O}^{2-}$  atoms, from EPC [ $\text{Rb}^{+}$ :  $12g \times 1$ ;  $\text{Ti}^{4+}$ :  $6e \times 1$ ;  $\text{Ge}^{4+}$ :  $6f \times 1 + 12g \times 1$ ;  $\text{O}^{2-}$ :  $2b \times 1 + 4d \times 1 + 6f \times 2 + 12g \times 3$ ]

## 4 Discussion and conclusion

### 4.1 Discussion

Incremental computation of objective functions, including the more elaborate ones (*eg.* those involving coordination numbers and valences), should be readily applicable to programs that mainly use atomic coordinates as the structural parameters for the optimisation algorithm, *eg.* *FOX* (Favre-Nicolin & Černý 2002) and *FraGen* (Li, Yu & Xu 2012); nevertheless, this technique is perhaps not trivially usable in direct space method programs that mainly specialise in molecular crystals, *eg.* *EXPO* (Altomare, Cuocci, Giacovazzo, Moliterni, Rizzi, Corriero & Falcicchio 2013), because of the heavy use of bond lengths, bond angles, *etc.* in the independent variables, where even a single change in one parameter might affect all atomic coordinates.

Even though most crystallographic software do not employ the EPC method, parallelisable tasks are widespread: *eg.* for SDPD of complicated structures, it is often necessary to run the optimisation algorithm several times before picking a best result (*cf.* Subsection 3.3), and these runs are trivially parallelisable, similar to the situation in Subsection 2.4. Parallelisation of optimisation algorithms can also be useful: *eg.* by parallelising the algorithms used in structure refinement, we would be able to dramatically reduce the time spent by the user on waiting for the results; we note that the recent work by Eremenko, Krayzman, Gagin & Levin (2017) is already in this direction.

As demonstrated in Section 3, apart from *a posteriori* structure validation and real-time elimination of crystallographic models with atom bumping, the atom bumping evaluation function can also be used in automatic *a priori* filtering of EPCs that cannot produce reasonable models at all. Filtering using other evaluation functions, *eg.* those that evaluate the goodness of bonding relations in crystallographic models, should also be usable in principle, and will surely be of interest: *eg.* with such advanced filtering, the manual steps in Subsection 3.3 could be greatly simplified.

As mentioned in Section 3, even with *a priori* filtering of EPCs that would produce unreasonable crystallographic models, and with the objective function employing anti-bump constraints, we might still get solutions with atom bumping. We think this is because certain EPCs just cannot produce models with small Bragg *R* factors without introducing atom bumping, or can but only with a very small probability. For this reason, we still need to perform *a posteriori* filtering of solutions with atom bumping.

### 4.2 Conclusion

We presented *decryst*, an open source software suite for crystal structure determination from powder diffraction data. *decryst* can offer high performance due to the application of incremental computation, and the performance can be further enhanced by using its features for parallel and distributed computing. *decryst* is simple yet flexible, and we explicitly wish the underlying techniques to be adopted in more crystallographic applications.

## Acknowledgements

The author is deeply indebted to all users that participated in the testing of *decryst*, whose suggestions were invaluable to the documentation of the software. The author would also like to thank Cheng Dong for bringing up the issue of crystallographic collision detection, thank the Bilbao Crystallographic Server (Aroyo, Perez-Mato, Capillas, Kroumova, Ivantchev, Madariaga, Kirov & Wondratschek 2006) for kindly providing crystallographic data in the spirit of open access, and thank the anonymous referees for their enlightening comments. This article is dedicated to Pieter Hintjens (1962.12.3 – 2016.10.4), a main author of *ZeroMQ*, the message passing library used in the implementation of parallel simulated annealing in *decryst*. This project was supported by the National Natural Science Foundation of China under grant No. 21271183.

## References

- Altomare, A., Cuocci, C., Giacovazzo, C., Moliterni, A., Rizzi, R., Corriero, N. & Falcicchio, A. (2013), ‘Expo2013: a kit of tools for phasing crystal structures from powder data’, *J. Appl. Cryst.* **46**(4), 1231–1235.
- Aroyo, M. I., Perez-Mato, J. M., Capillas, C., Kroumova, E., Ivantchev, S., Madariaga, G., Kirov, A. & Wondratschek, H. (2006), ‘Bilbao crystallographic server i: Databases and crystallographic computing programs’, *Z. Kristallog.* **221**(1), 15–27.
- Baerlocher, C., McCusker, L. B. & Palatinus, L. (2006), ‘*Ab initio* structure solution from powder diffraction data using charge flipping’, *Acta. Cryst.* **A62**(A1), s231.
- Bryant, R. E. & O’Hallaron, D. R. (2011), *Computer Systems: A Programmer’s Perspective*, 2 edn, Pearson, Boston, MA, p. 46.
- Chu, K.-W., Deng, Y.-F. & Reinitz, J. (1999), ‘Parallel simulated annealing by mixing of states’, *J. Comput. Phys.* **148**(2), 646–662.
- David, W. I. F., Shankland, K., McCusker, L. B. & Baerlocher, C., eds (2002), *IUCr Monographs on Crystallography, Volume 13: Structure Determination from Powder Diffraction Data*, Oxford University Press, Oxford, UK.
- Deng, X.-D. & Dong, C. (2009), ‘Smepoc: a computer program for the automatic generation of trial structural models for inorganic compounds with symmetry restriction’, *J. Appl. Cryst.* **42**(5), 953–958.
- Deng, X.-D. & Dong, C. (2011), ‘Epcryst: a computer program for solving crystal structures from powder diffraction data’, *J. Appl. Cryst.* **44**(1), 230–237.
- Downs, R. T. & Hall-Wallace, M. (2003), ‘The american mineralogist crystal structure database’, *Am. Mineral.* **88**(1), 247–250.
- Eremenko, M., Krayzman, V., Gagin, A. & Levin, I. (2017), ‘Advancing reverse monte carlo structure refinements to the nanoscale’, *J. Appl. Cryst.* **50**(6), 1561–1570.
- Favre-Nicolin, V. & Černý, R. (2002), ‘Fox, ‘free objects for crystallography’: a modular approach to ab initio structure determination from powder diffraction’, *J. Appl. Cryst.* **35**(6), 734–743.
- Feldman, S. I. (1979), ‘Make – a program for maintaining computer programs’, *Softw.: Pract. Exper.* **9**(4), 255–265.
- Higham, N. J. (1993), ‘The accuracy of floating point summation’, *SIAM J. Sci. Comput.* **14**(4), 783–799.
- Kahan, W. (1965), ‘Further remarks on reducing truncation errors’, *Commun. ACM* **8**(1), 40.
- Lam, J. & Delosme, J.-M. (1988), An efficient simulated annealing schedule: Implementation and evaluation, Technical Report 8817, Department of Electrical Engineering, Yale University.
- Li, Y., Yu, J.-H. & Xu, R.-R. (2012), ‘Fragen: a computer program for real-space structure solution of extended inorganic frameworks’, *J. Appl. Cryst.* **45**(4), 855–861.
- Liu, Y. (2017), ‘Real-time detection and resolution of atom bumping in crystallographic models (arxiv:1708.03180)’, *Acta. Cryst.* **A73**(5), 414–422.
- Lu, H.-S. & Liang, C.-K. (1965), ‘The crystal structure of  $v_2ga_5$ ’, *Acta Phys. Sin.* **21**(5), 997–1007.

Reddy, J. M., Storm, A. R. & Knox, K. (1965), ‘The crystal structure of  $\text{v}_2\text{ga}_5$ ’, *Z. Kristallog.* **121**(6), 441–448.

Černý, R. & Favre-Nicolin, V. (2007), ‘Direct space methods of structure determination from powder diffraction: principles, guidelines and perspectives’, *Z. Kristallog.* **222**(3/4), 105–113.